

OpenSpectro: An Open-Source Spectroscopic Profiling Platform

Haoran Zhang*, Elizabeth C. Courtney*, Kyle C. Quinn⁺ and Amanda Watson*

* Department of Electrical and Computer Engineering, University of Virginia

⁺ Department of Anesthesiology, University of Virginia

Abstract—Spectroscopic analysis is essential for identifying optical molecular signatures, which are distinct patterns observed across different wavelengths. Understanding these signatures provides critical insights for designing wearable health-monitoring devices. In particular, constructing three-dimensional (3D) spectroscopic graphs of molecular spectra enables the optimization of multi-wavelength photoplethysmography (PPG) sensors, improving their accuracy and performance. However, no prior work has systematically mapped spectroscopic signatures to optimize wavelength combinations, slowing advancements in multi-wavelength PPG sensor deployment. To address this gap, we introduce OpenSpectro, an open-source spectroscopic profiling platform for visualizing and sharing molecular spectral data, particularly human physiological biomarkers. OpenSpectro features a preliminary spectroscopic database containing 17 biomarkers and a spectral attention optimization model that identifies customized wavelength attention weights for each biomarker.

I. INTRODUCTION

Aging society and rising healthcare costs have heightened the focus on preventive care and long-term body monitoring, prompting a surge of interest in wearable devices [1]. These devices provide continuous data that not only enables early disease detection but also facilitates the development of personalized healthcare solutions [2]. Traditional invasive methods such as blood sampling or implantable devices are often costly, painful, and yield only intermittent measurements [3]. Wearable technologies offer a low-cost, non-invasive, and continuous monitoring alternative that is highly appealing for both clinical and personal health applications [4]. Our primary objective is to eliminate the need for invasive sampling methods in medical devices by transitioning these technologies out of the confines of the clinical setting. This shift enhances patient comfort and accessibility, capturing longitudinal, real-time health data for personalized and proactive patient-centered healthcare.

Among the various technologies utilized in wearable devices, PPG stands out for its low cost, convenience, and high sampling rate [5]. It has been widely applied in monitoring blood pressure, blood glucose levels, blood oxygen saturation, heart rate, and drug delivery [6]–[10]. However, due to its susceptibility to interference including motion artifacts, ambient light variations, and the optical complexities of skin and blood [11], its adoption in clinical practice remains limited. Multi-wavelength PPG devices have demonstrated effectiveness in mitigating these interferences [5]. Recent research indicates that multi-wavelength PPG enables the discovery and monitoring of novel biomarkers such as hydration status and dyshemoglobins, significantly expanded its

clinical utility [12], [13]. Despite its potential, no comprehensive spectroscopic research has been conducted to optimize multi-wavelength PPG sensor development—a critical gap this work seeks to address. To overcome these limitations, we trained a spectral attention optimization model using spectroscopic data to optimize activation wavelengths.

This paper addresses the following key research questions:

- RQ1: How can a spectroscopic platform enhance the identification of unique molecular signatures and improve the specificity and accuracy of biomarker detection?
- RQ2: How can spectroscopic data inform the optimization of excitation wavelengths and photodetector configurations in wearable devices?

The OpenSpectro¹ platform enables interactive exploration of molecular spectral signatures across intensity, absorbance, and fluorescence domains, augmented by contextual metadata such as biomarker concentration, solvent conditions, and algorithmically derived optimal detection wavelengths. By providing standardized access of these profiles, researchers can systematically identify target substances and gain actionable insights to optimize wavelength configurations, bridging the gap between spectral analysis and hardware design.

Complementing the platform, we developed a spectral attention optimization algorithm that identifies wavelength attention weights using constrained gradient-based optimization. This model learns sparse, interpretable attention weights by maximizing correlations with target biomarkers while explicitly penalizing wavelengths prone to interference from overlapping spectral signatures. Unlike traditional approaches that rely on fixed, non-adaptive wavelength combinations—which often include redundant or noisy channels—our model generates customized configurations tailored to specific biomarkers.

The primary contributions of this work are:

- PC1: OpenSpectro, an open-source platform that integrates spectroscopic profiles of 17 biomarkers, enabling interactive molecular spectral signature visualization.
- PC2: A wavelength optimization model that leverages spectral profiles to streamline the design of PPG devices, enhancing both their precision and functionality.

The remainder of this paper is structured as follows: Section II presents our motivation and reviews related work. Section III outlines the system architecture of OpenSpectro and the theoretical framework underlying its operation. In Section

¹Visit OpenSpectro at openspectro.github.io.

TABLE I: Biomarkers tested

ID	Biomarker Name	Chemical Formula	Concentration	Source	Bio-function
1	Bilirubin	$C_{33}H_{36}N_4O_6$	1.67 mg/mL	Human	Byproduct of red blood cell breakdown
2	C-Reactive Protein (Human)	$C_{38}H_{57}N_9O_8$	100.0 μ L/mL	Human	Marker of inflammation
3	Collagen	$C_{57}H_{91}N_{19}O_{16}$	4.00 mg/mL	Human	Structural support to the connective tissues
4	Creatinine	$C_4H_7N_3O$	10.00 mg/mL	Chem	Waste product of muscle metabolism
5	Ghrelin	$C_{149}H_{248}IN_{47}O_{42}$	13.33 mg/mL	Human	Stimulates hunger, regulates energy
6	Glucose	$C_6H_{12}O_6$	25.00 μ L/mL	Human	Primary energy source for cells
7	Hemoglobin A_e	$C_{2952}H_{4464}N_{3248}O_{812}S_8Fe_4$	3.33 mg/mL	Human	Transports oxygen from the lungs
8	Hemoglobin Human	$C_{2952}H_{4464}N_{3248}O_{812}S_8Fe_4$	5.00 mg/mL	Human	Transports oxygen from the lungs
9	High Density Lipoprotein	$C_{27}H_{46}O$	500.0 μ L/mL	Human	Transports cholesterol to liver
10	Human Leptin	$C_{87}H_{138}N_{22}O_{28}S_2$	0.50 mg/mL	Animal	Regulates energy balance
11	Insulin	$C_{256}H_{381}N_{65}O_{77}S_6$	2.50 mg/mL	Synthesized	Regulates blood glucose levels
12	Melatonin	$C_{13}H_{16}N_2O_2$	2.00 mg/mL	Animal	Endocrine rhythm regulation
13	Sodium Lactate	$C_3H_5NaO_3$	20.00 mg/mL	Chem	Electrolyte replenisher buffering agent
14	Tryptophan	$C_{11}H_{12}N_2O_2$	1.33 mg/mL	Human	Precursor for serotonin, melatonin
15	Tyrosine	$C_9H_{11}NO_3$	0.70 mg/mL	Animal	Precursor for neurotransmitters
16	Urea	CH_4N_2O	100.0 mg/mL	Chem	Waste product formed in the liver
17	Very Low Density Lipoprotein	$C_{55}H_{98}O_6$	0.30 mg/mL	Human	Transports triglycerides and cholesterol

IV, we display 3D spectroscopic graphs and demonstrate the optimization of wearable sensor wavelengths. Finally, Section V summarizes our findings and future work.

II. MOTIVATION AND RELATED WORK

A. Motivation

Wearable monitoring devices employ various sensing technologies, including inertial measurement units (IMUs), impedance sensing, electromyography (EMG), and photoplethysmogram (PPG) [14]. This paper focuses on PPG as a tool for analyzing physiological biomarkers. Most existing PPG systems rely on single-peak wavelengths for target analysis [15], whereas multi-wavelength PPG enables more precise tracking of specific molecular signatures [5].

A rarely explored aspect of wearable spectroscopic analysis is fluorescence, where certain substances emit light at different wavelengths when excited by specific wavelengths. This process occurs when electrons absorb energy, jump to a higher energy level, and then release the energy as emitted light [16]. For example, bilirubin has been shown to fluoresce with an excitation maximum near 476 nm and emission detected around 530 nm, with the most effective phototherapy range being 460–490 nm [17]. These fluorescing biomarkers introduce new possibilities for wearable devices that can detect and analyze emission-based signatures. However, traditional two-dimensional (2D) spectroscopic scans can only visualize spectral data at matching wavelengths, potentially missing important fluorescence. A full three-dimensional (3D) spectroscopic scan is crucial for capturing fluorescence and ensuring a more comprehensive analysis.

Capturing such broad-spectrum data requires advanced experimental setups, including tunable lasers and high-resolution spectrometers, making these studies rare in conventional spectroscopic research. To bridge this gap, OpenSpectro serves as a preliminary spectroscopic profiling platform, providing detailed spectroscopic signatures of various substances. By offering optimized wavelength selection for light emitting diodes (LEDs) and photodetectors (PDs),

OpenSpectro streamlines the design of wearable multi-wavelength PPG devices, enhancing both their precision and functionality. Through detailed spectroscopic profiling, OpenSpectro advances the study of molecular responses, promoting the development of next-generation wearable health technologies and more accurate biomarker detection.

The closest spectral profiling research related to our work is the HITRAN molecular absorption database [18], which provides comprehensive spectroscopic parameters primarily for atmospheric and remote-sensing applications. However, its focus is on environmental and planetary contexts rather than biomedical or wearable-device use cases.

B. Multi-wavelength PPG

Recent advances in multi-wavelength PPG extend its utility beyond conventional pulse oximetry to diverse physiological measurements [19]. Blood oxygen saturation (SpO₂) and heart rate (HR) estimation, traditionally reliant on red-infrared (IR) wavelengths, now benefit from green-orange wavelengths (525–595 nm), which exhibit superior motion robustness ($r = 0.98$ – 0.99 correlation with reference devices) [6], [20]. Multi-wavelength PPG also enables non-invasive blood pressure (BP) monitoring by leveraging pulse transit time (PTT) differences across wavelengths [7]. Similarly, blood glucose (BG) estimation improves with multi-wavelength fusion, achieving a 6.16 mg/dL prediction error using green-red-IR combinations [8]. These studies highlight multi-wavelength synergies over single-peak approaches, particularly in mitigating motion artifacts.

Despite these advancements, challenges persist in standardizing wavelength selection, managing inter-device variability, and reducing calibration dependencies [5]. A key limitation of multi-wavelength PPG is wavelength overlap among biomarkers, causing cross-interference [21]. Thus, simply increasing the number of wavelengths is insufficient; instead, targeted wavelength selection and advanced models are essential for effectively processing spectral data. Advances in computing and machine learning now extract meaningful insights from high-fidelity spectroscopic data,

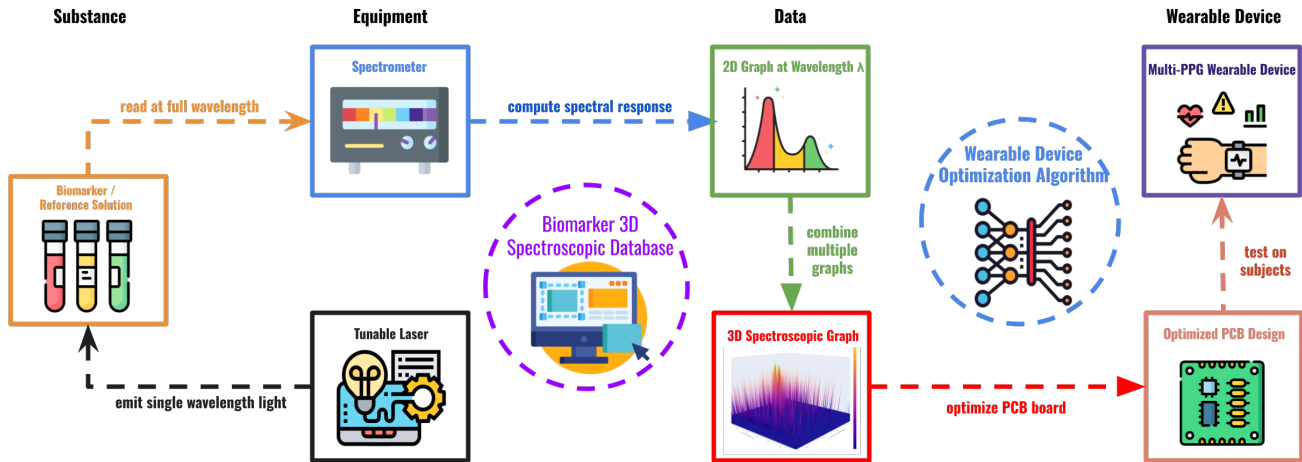


Fig. 1: OpenSpectro system architecture

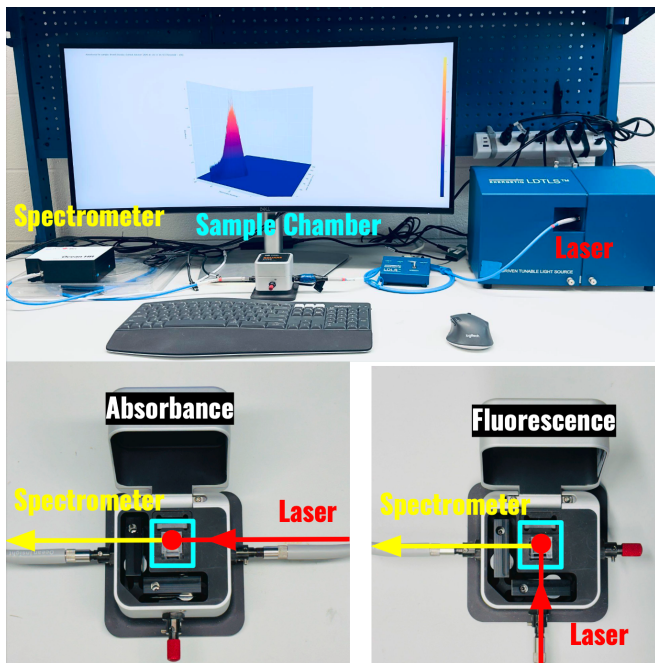


Fig. 2: Experimental setup

overcoming prior multi-wavelength PPG constraints [22], [23]. However, no prior research has systematically mapped spectroscopic signatures to optimize wavelength combinations for multiple biomarkers—an essential gap that OpenSpectro’s model aims to address.

III. OPENSPECTRO SYSTEM

Here we present the OpenSpectro system in detail, as shown in Figure 1. First, we describe the equipment used to collect absorption and fluorescence spectra. Next, we outline the measurement function applied during data acquisition. Finally, we demonstrate the theoretical foundation of the optimization algorithm.

A. Equipment Setup

In order to develop a database of biomarkers in isolation, we leveraged a tunable light source, high-resolution spectrometer, and a sample chamber as shown in Figure 2. For the light source, we selected Energetiq’s TLS-EQ-9-S, a flexible wavelength tunable light source. It operates from 380 nm to 1100 nm allowing highly specific wavelength selection for targeted spectral analysis. The OceanOptics HR6 Spectrometer covers the ultraviolet, visible, and near-infrared ranges, with a wavelength range from 180 nm to 1100 nm and an optical resolution between 0.08 nm and 7.24 nm. Before profiling, the sample was diluted and placed into Eppendorf cuvettes. For absorbance, the laser and spectrometer were aligned in a straight path. For fluorescence, they were aligned in an orthogonal orientation. Each scan took approximately 90 minutes to complete.

B. Spectral Profiling

To profile a sample, we developed a custom API control application leveraging our laser and spectrometer. This application allows for stepwise adjustment of the laser wavelength and real-time acquisition of spectrometer readings across the full spectral range. By leveraging this capability, we generate three-dimensional visualizations of spectral responses, enabling characterization of absorbance, fluorescence, and phosphorescence within a single representation. The workflow involves the following steps:

Sample Preparation/Dilution: A solution was prepared by dissolving our targeted biomarker, known as the analyte, into a liquid medium, called the solvent, to facilitate measurement. In most cases, the analyte was diluted using a Phosphate Buffered Saline (PBS) solution which maintains a pH similar to that of blood, ensuring a physiologically relevant environment for analysis. The solution was placed into Eppendorf cuvettes that were inserted into our sample chamber. The analyte concentrations were carefully prepared to span a physiologically relevant detection range, with the

corresponding values listed in Table I. Some biomarkers were supplied in aqueous form, lacking initial concentration data. Their diluted concentrations are given in $\mu\text{L}/\text{mL}$ as biomarker-to-buffer ratios.

Spectral Profiling: Absorbance (A) quantifies how much light at a specific wavelength λ is absorbed by a sample as it passes through. Absorbance is calculated by comparing the intensity of light that passes through the sample to that of a reference sample (PBS) while accounting for background noise. It can be calculated using the formula:

$$A_\lambda = -\log_{10}\left(\frac{S_\lambda - B_\lambda}{R_\lambda - B_\lambda}\right) \quad (1)$$

where S_λ is the intensity of the analyte sample at wavelength λ , B_λ is the intensity of the background at wavelength λ , and R_λ is the intensity of the reference sample at wavelength λ . The influence of the Eppendorf cuvettes has been eliminated by also using them for the PBS sample. This equation accounts for background subtraction to ensure that only the analyte's absorbance is measured, reducing noise from environmental and instrumental factors. The logarithmic transformation provides a direct relationship between absorbance and concentration.

Fluorescence is the process in which a substance absorbs light at one wavelength and emits it at an alternative wavelength. Unlike absorbance, which measures the reduction in light intensity as it passes through a sample, fluorescence detection captures the emitted light from an excited analyte. After changing the orientation of the device (Figure 2), we use the similar function as Equation 1 to calculate fluorescence at wavelength λ (F_λ) by:

$$F_\lambda = -\log_{10}\left(\frac{R_\lambda - B_\lambda}{S_\lambda - B_\lambda}\right) \quad (2)$$

where S_λ is the intensity of the analyte sample at wavelength λ , B_λ is the intensity of the background at wavelength λ and R_λ is the intensity of the reference sample at wavelength λ . The influence of the Eppendorf cuvettes has been removed from the spectra by using it for the PBS sample as well. This calculation accounts for background subtraction to ensure that only the fluorescence signal is captured. The logarithmic transformation standardizes the fluorescence intensity, improving reliability of comparisons across samples.

Noise Reduction and Threshold Filtering: To minimize issues such as logarithmic explosions and background noise, filtering and thresholding are applied:

$$A_\lambda = \begin{cases} 0 & S_\lambda \geq R_\lambda, R_\lambda - S_\lambda \leq \tau \\ & \text{or } S_\lambda - B_\lambda \leq \tau \\ -\log_{10}\left(\frac{S_\lambda - B_\lambda}{R_\lambda - B_\lambda}\right) & \text{otherwise} \end{cases} \quad (3)$$

where τ is the threshold value to exclude small differences between the numerator and denominator. Specifically, if the intensity differences between the sample and reference ($R_\lambda - S_\lambda$) or the sample and background ($S_\lambda - B_\lambda$) are

too small (i.e., below a threshold τ), absorbance is set to zero to avoid numerical artifacts. This approach ensures that meaningful changes are captured while filtering out insignificant or noisy variations. Similar thresholding is also applied to fluorescence readings.

C. Wearable Devices Optimization Algorithm

The wearable device optimization feature enables users to select biomarkers of interest and generates conceptual designs tailored to the selected biomarkers. By integrating 2D and 3D spectroscopic analyses, this tool bridges the gap between molecular insights and practical device development.

2D Spectroscopic Optimization: Consider a system with N biomarkers, each represented by an absorbance spectrum of length M . Let $A \in \mathbb{R}^{N \times M}$, where the i -th row $A_i = (A_{(i,1)}, A_{(i,2)}, \dots, A_{(i,M)})$ denotes the absorbance values of the i -th biomarker across M wavelengths. Therefore, to enhance the detection of a biomarker i , we define an attention vector:

$$\mathbf{w}_i = (w_{(i,1)}, w_{(i,2)}, \dots, w_{(i,M)}) \in [0, 1]^M \quad (4)$$

where $w_{(i,m)}$ represents the attention weight for wavelength m of biomarker i . To focus on target biomarker i while minimizing interference from others, we introduced:

$$\mathcal{L}_i(\mathbf{w}) = \alpha \sum_{m=1}^M w_{(i,m)} A_{(i,m)} - \beta \sum_{j=1, j \neq i}^N \sum_{m=1}^M w_{(i,m)} A_{(j,m)} \quad (5)$$

where $\alpha > 0$ emphasizes the target biomarkers by assigning higher weights to wavelengths where absorbance is strongest. $\beta > 0$ penalizes interference from others $j \neq i$ by reducing the weights at overlapping wavelengths. The goal is to maximize $\mathcal{L}(\mathbf{w})$ while ensuring that the attention weights remain within valid bounds $\mathbf{w} \in [0, 1]^{N \times M}$:

$$\max_{\mathbf{w}_i \in [0, 1]^M} \sum_{i=1}^N \mathcal{L}_i(\mathbf{w}) \quad (6)$$

This ensures that the selected wavelengths maximize sensitivity to the target biomarker while minimizing spectral interference from other biomarkers. By optimizing \mathbf{w} , this approach improves detection of the target biomarker and reduces spectral overlap, making it well-suited for wearable device applications where the targeted environment is crowded with background noise and interfering signals.

3D Spectroscopic Optimization: In 3D spectroscopic scanning, we combine absorbance and fluorescence readings into a single 3D spectral map to enhance biomarker characterization. While fluorescence maybe rare, it is a unique property that can be leveraged to distinguish specific biomarkers from others, providing an additional dimension for spectral differentiation and enhancing detection accuracy. Typically, absorbance values are located along the diagonal, where the LED and photodetector (PD) wavelengths match, while fluorescence readings are positioned off-diagonal.

We define the spectral response system as: $S \in \mathbb{R}^{N \times M_1 \times M_2}$, where $S_{(i,:,:)}$ represents the absorbance and fluorescence values of the i -th biomarker across M_1 LED

wavelengths (excitation sources) and M_2 represents PD wavelengths (detection wavelengths). For each biomarker, we define the attention matrix:

$$\mathbf{W}_i \in [0, 1]^{M_1 \times M_2} \quad (7)$$

where $W_{(i,u,v)}$ represents the attention weight at LED index u and PD index v for biomarker i . Thus, the objective function for emphasizing target biomarker i while minimizing interference is:

$$\mathcal{L}_i(\mathbf{W}) = \alpha \sum_{u=1}^{M_1} \sum_{v=1}^{M_2} W_{(i,u,v)} S_{(i,u,v)} - \beta \sum_{\substack{j=1 \\ j \neq i}}^N \sum_{u=1}^{M_1} \sum_{v=1}^{M_2} W_{(i,u,v)} S_{(j,u,v)} \quad (8)$$

where $\alpha > 0$ enhances sensitivity to the target biomarker i by assigning higher weights to wavelengths where its absorbance and fluorescence signals are strongest. Conversely, $\beta > 0$ penalizes interference from other biomarkers $j \neq i$ by reducing weights at overlapping wavelengths. This formulation ensures that the selected wavelengths maximize sensitivity to the target biomarker while minimizing spectral interference from others.

IV. RESULTS

A. OpenSpectro Platform

To accelerate advancements in wearable health monitoring technology, we developed OpenSpectro, an open-source, online platform for spectroscopic profiling. Designed for researchers, engineers, and clinicians, it offers a collaborative, accessible, and extensible tool for analyzing spectroscopic data. Built using Python’s Flask framework, OpenSpectro features interactive 3D graphs displaying absorbance, fluorescence, and raw intensity spectra for the 17 biomarkers shown in Table I with ongoing expansions. Each dataset includes metadata, including concentration levels, solvent type, color representation, major biological functions, chemical formulas, and molecular structures.

OpenSpectro enables users to integrate spectroscopic data in a variety of ways. It compares absorbance versus fluorescence, helping to identify peak wavelengths and off-diagonal fluorescence emissions that are overlooked in conventional two-dimensional analysis. Additionally, it supports the optimization of multi-wavelength sensor design by generating customized LED and photodetector configurations for wearable biomarker detection. By analyzing overlapping spectra, OpenSpectro helps detect the degree of obscuring between biomarkers (for instance, glucose and hemoglobin at 510 nm) and refines multi-wavelength PPG algorithms. Beyond biomedical applications. It can be adapted for environmental sensing, material characterization, and industrial uses.

B. Spectroscopic Optimization

Using the 17 biomarkers we scanned in Table I, we applied the optimization algorithm described in Section III to generate optimized multi-wavelength PPG wavelength

graphs. This graph shown at the bottom of Figure 3, illustrates attention weights that highlight the significance of specific PD and LED wavelengths. To improve readability and clarity in the visualization, we limited the spectrum to the visible light range (425 nm to 600 nm) and selected five representative wavelengths per biomarker, ensuring that the chosen wavelengths are well-spaced and clearly labeled. Since fluorescence was infrequently detected in our dataset, we focus on the 2D optimization for our analysis. In future work, once more biomarkers with fluorescence are identified, we will expand this analysis to the 3D optimization.

Our model employs a specialized 2D attention layer that assigns attention weights to each biomarker across the wavelength range. The layer is trained using the spectral loss function defined in Equation 5, with hyper-parameter set to $\alpha = 1.0$ and $\beta = 0.5$, ensuring a balance between enhancing the target biomarker signal and minimizing interference from other biomarkers. The Adam optimizer ($lr = 10^{-2}$) is employed for parameter updates.

The three evaluation metrics for each biomarker are presented in Table II, namely *Target*, *Interference*, and *Detection Effectiveness*. The *Target* column records the sum of the dot product between the attention vector and the corresponding biomarker’s absorbance values, representing the correlation between the trained attention weights and the absorbance values of the target biomarker. The *Interference* column records the sum of the dot product between the attention vector and all other biomarkers absorbance values, reflecting the degree of spectral overlap between the learned attention weights and non-target biomarkers. To quantify the effectiveness of the learned attention weights, we define a performance metric named *Detection Effectiveness*, $DE(\mathbf{w}_i)$ as follows:

$$DE(\mathbf{w}_i) = \frac{\text{Target}}{\sqrt{\text{Interference}}} = \frac{\sum_{m=1}^M w_{(i,m)} A_{(i,m)}}{\sqrt{\sum_{\substack{j=1 \\ j \neq i}}^N \sum_{m=1}^M w_{(i,m)} A_{(j,m)}}} \quad (9)$$

An ideal trained model would achieve high *Target* value (strong correlation with the intended biomarker) and low *Interference* value (minimal overlap with other biomarkers), which results in high *DE* metric. Table II summarizes performance across all scanned biomarkers. Hemoglobin, VLDL, and Glucose have the highest *Target* values (6.41, 7.84, and 5.11) with high *DE* values (0.62, 0.83, and 0.55). Urea, Tyrosine, and Insulin have the lowest *Target* values (0.90, 0.72, and 1.06) and low *DE* values (0.23, 0.21, and 0.25). Ghrelin shows no absorbance in our wavelength range, with a target absorbance of 0.0. Biomarkers with a *Target* value less than 4.0 like Bilirubin, Insulin, and Lactate can be improved by expanding wavelength range to NIR.

For example, in the case of HemoglobinAe, the absorbance peaks occur around 530 nm and 572 nm. However, Glucose also exhibits high absorbance near 530 nm, leading to a reduced attention weight for HemoglobinAe in that region. Instead, the optimization shifts emphasis toward 572 nm, where spectral overlap is minimal. This behavior demonstrates how the algorithm adaptively avoids interference, and

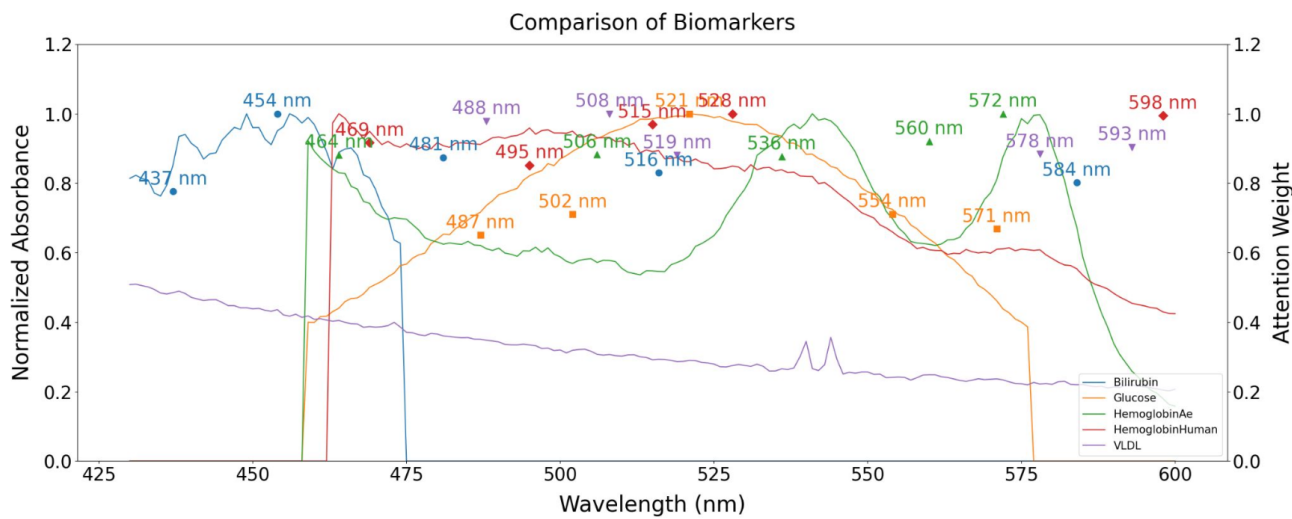
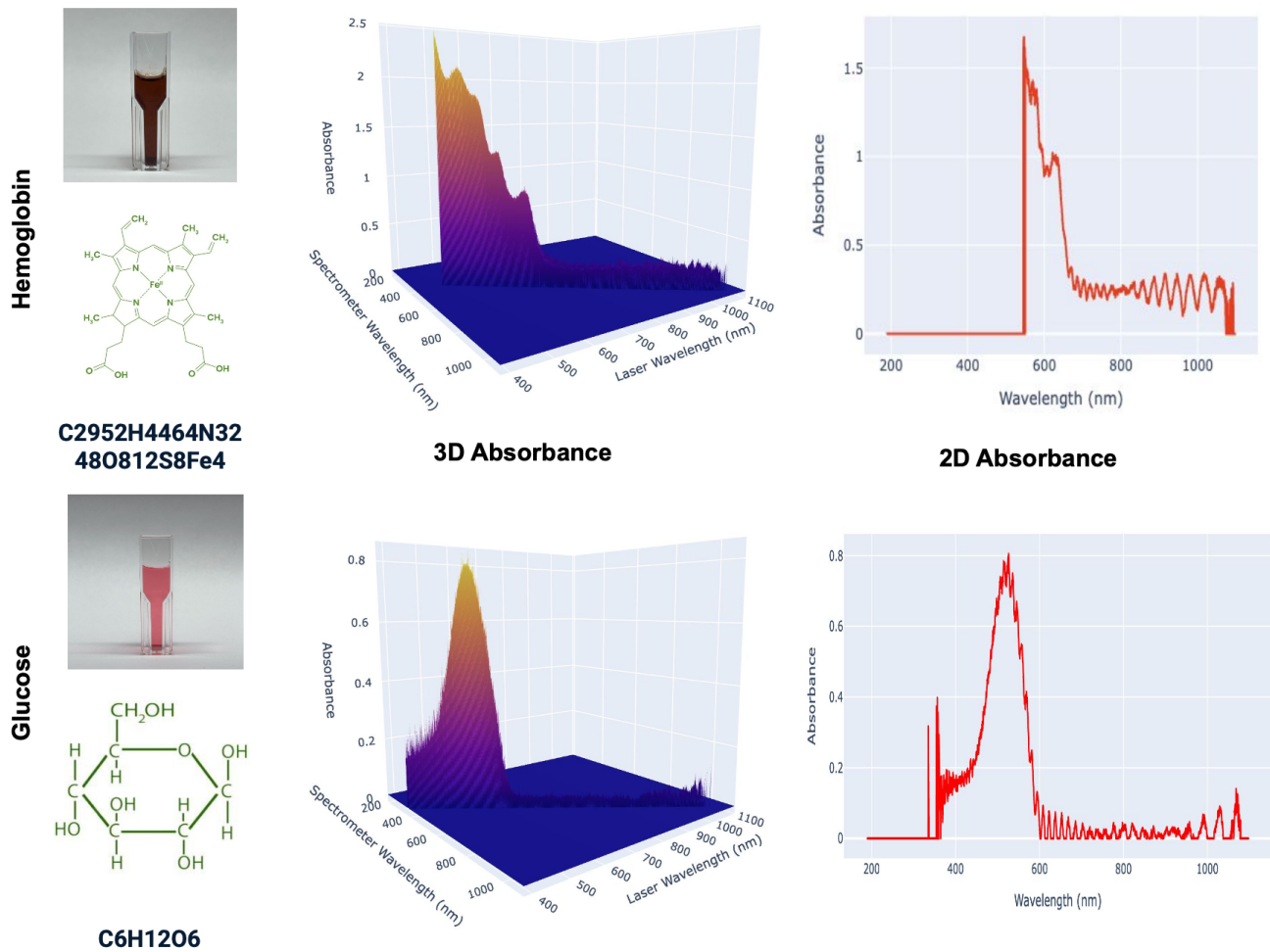


Fig. 3: OpenSpectro visualization example and spectral optimization result

TABLE II: Optimization result

ID	Biomarker Name	Target	Interference	DE
1	Bilirubin	2.53	42.60	0.39
2	C-Reactive Protein	2.48	41.90	0.38
3	Collagen	1.25	21.10	0.27
4	Creatinine	1.43	24.21	0.29
5	Ghrelin	0.00	0.00	NA
6	Glucose	5.11	86.39	0.55
7	HDL	2.07	35.08	0.35
8	Hemoglobin A_2	4.15	70.00	0.50
9	Hemoglobin Human	6.41	108.2	0.62
10	Human Leptin	2.46	41.65	0.38
11	Insulin	1.06	17.94	0.25
12	Melatonin	1.82	30.76	0.33
13	Sodium Lactate	3.57	60.32	0.46
14	Tryptophan	3.50	59.32	0.45
15	Tyrosine	0.72	12.22	0.21
16	Urea	0.90	15.12	0.23
17	VLDL	7.84	89.61	0.83

we anticipate even more robust performance as additional biomarker data are incorporated and wavelength proximity constraints are integrated into the objective function. Some biomarkers, such as Bilirubin, exhibit very low absorbance within our spectrometer’s operating range but are known to fluoresce. This quality is expected to improved the wavelength identification for such biomarkers.

V. CONCLUSION AND FUTURE WORK

In this paper, we introduced OpenSpectro, a comprehensive platform that integrates a database of 17 biomarkers and an optimization algorithm for optical-based wearable devices. OpenSpectro features interactive 3D spectroscopic graphs, enabling users to explore intensity, fluorescence (in the future), and absorption spectra in detail. The insights provided by OpenSpectro contribute to the advancement of future wearable device development and facilitate the tracking of fluorescence in addition to absorption, expanding the capabilities of bio-sensing technologies.

While OpenSpectro offers a strong foundation, several limitations and opportunities for improvement remain. Currently comprehensive fluorescence detection is limited by lack of appropriate equipment for optical filtering and proper excitation-emission separation, but future modifications plan to incorporate optical filters and optimized detection geometry. Additionally, the wavelength selection algorithm does not yet factor in wavelength distance constraints, which can lead to spectral overlap, nor does it account for biomarker concentration difference in the body.

Further advancements of this research include expanding the spectral range into the infrared region, integrating additional methods such as Raman spectroscopy for molecular analysis, and leveraging deep learning for molecular spectrum prediction. A key next step is to conduct real-world user studies using wearable devices such as Lumos [10] optimized via our platform for biomarker detection. Additionally, exploring molecular interactions and spectral analysis of complex mixtures, such as glycosylated hemoglobin (HbA1c), could enhance medical diagnostics and reduce drug monitoring costs. By incorporating deep

learning techniques, OpenSpectro could predict unmeasured molecular spectra, future advancing its role in medical discovery and non-invasive health monitoring. Through these innovations, OpenSpectro contributes to the future of optical based wearable technology, expanding the capabilities of bio-sensing devices beyond their current limitations.

REFERENCES

- [1] S. Madanian, H. H. Nguyen, and F. Mirza, “Wearable technology,” in *Encyclopedia of gerontology and population aging*. Springer, 2022.
- [2] F. Haghayegh, A. Norouziyazad *et al.*, “Revolutionary point-of-care wearable diagnostics for early disease detection and biomarker discovery through intelligent technologies,” *Advanced Science*, 2024.
- [3] K. Bazaka and M. V. Jacob, “Implantable devices: issues and challenges,” *Electronics*, 2012.
- [4] S. Iqbal, I. Mahgoub, E. Du, M. Leavitt, and W. Asghar, “Advances in healthcare wearable devices,” *NPJ Flexible Electronics*, 2021.
- [5] D. Ray, T. Collins, S. Woolley, and P. Ponnappalli, “A review of wearable multi-wavelength photoplethysmography,” *IEEE Reviews in Biomedical Engineering*, 2021.
- [6] S. Alharbi, S. Hu, D. Mulvaney, L. Barrett, L. Yan *et al.*, “Oxygen saturation measurements from green and orange illuminations of multi-wavelength optoelectronic patch sensors,” *Sensors*, 2018.
- [7] J. Liu, Y. Li, X. Ding *et al.*, “Effects of cuff inflation and deflation on pulse transit time measured from eeg and multi-wavelength ppg,” in *IEEE Engineering in Medicine and Biology Society*, 2015.
- [8] V. Rachim and W. Chung, “Wearable-band type visible-near infrared optical biosensor for non-invasive blood glucose monitoring,” *Sensors and Actuators B: Chemical*, 2019.
- [9] P. Adhikari, I. Magaña, and P. O’Neal, “Multi-wavelength pulse-plethysmography for real-time drug delivery monitoring,” in *Optical Diagnostic & Sensing: Toward Point-of-Care Diagnostic*. SPIE, 2014.
- [10] A. Watson, C. Kendell, A. Lingamoorthy, I. Lee *et al.*, “Lumos: An open-source device for wearable spectroscopy research,” *ACM Interactive, Mobile, Wearable and Ubiquitous Technologies*, 2023.
- [11] R. Spetlík, J. Cech, and J. Matas, “Non-contact reflectance ppg: Progress, limitations, and myths,” in *International Conference on Automatic Face & Gesture Recognition (FG 2018)*. IEEE, 2018.
- [12] E. Volkova, A. Perchik, K. Pavlov, E. Nikolaev *et al.*, “Multispectral sensor fusion in smartwatch for in situ continuous monitoring of human skin hydration and body sweat loss,” *Scientific Reports*, 2023.
- [13] V. Lychagov, V. Semenov, E. Volkova, Chernakov *et al.*, “Non-invasive hemoglobin concentration measurements with multi-wavelength reflectance mode ppg sensor and cnn data processing,” in *45th IEEE Engineering in Medicine & Biology Society (EMBC)*, 2023.
- [14] G. Iadarola, A. Mengarelli, P. Crippa, S. Fioretti, and S. Spinsante, “A review on assisted living using wearable devices,” *Sensors*, 2024.
- [15] D. Castaneda, A. Esparza, M. Ghamari *et al.*, “A review on wearable ppg sensors and their potential future applications in health care,” *International journal of biosensors & bioelectronics*, 2018.
- [16] S. G. Schulman, *Fluorescence and phosphorescence spectroscopy: physicochemical principles and practice*. Elsevier, 2017.
- [17] A. Lamola and M. Russo, “Fluorescence excitation spectrum of bilirubin in blood: a model for the action spectrum for phototherapy of neonatal jaundice,” *Photochemistry and photobiology*, 2014.
- [18] I. Gordon, L. Rothman, C. Hill, R. Kochanov, Y. Tan, P. Bernath, M. Birk *et al.*, “The hitran2016 molecular spectroscopic database,” *Journal of quantitative spectroscopy and radiative transfer*, 2017.
- [19] T. Tamura, “Current progress of photoplethysmography and spo2 for health monitoring,” *Biomedical engineering letters*, 2019.
- [20] S. Alharbi, S. Hu *et al.*, “An applicable approach for extracting human heart rate and oxygen saturation during physical movements using a multi-wavelength illumination optoelectronic sensor system,” in *SPIE Design and Quality for Biomedical Technologies XI*, 2018.
- [21] P. Ray and A. J. Steckl, “Label-free optical detection of multiple biomarkers in sweat, plasma, urine, and saliva,” *ACS sensors*, 2019.
- [22] X. Xiao, J. Yin, J. Xu, T. Tat, and J. Chen, “Advances in machine learning for wearable sensors,” *ACS nano*, 2024.
- [23] A. Soleimany, A. Amini, S. Goldman, D. Rus, S. Bhatia, and C. Coley, “Evidential deep learning for guided molecular property prediction and discovery,” *ACS central science*, 2021.